





RESEARCH ARTICLE

Afforestation can lower microbial diversity and functionality in deep soil layers in a semiarid region

Weibo Kong^{1,2,3}  | Xiaorong Wei^{1,2,4}  | Yonghong Wu⁵  | Mingan Shao^{1,2,4} | Qian Zhang⁶ | Michael J. Sadowsky^{6,7} | Satoshi Ishii^{6,7} | Peter B. Reich^{8,9}  | Gehong Wei¹ | Shuo Jiao¹ | Liping Qiu^{1,2,4} | Liling Liu¹

¹State Key Laboratory of Soil Erosion and Dryland Farming on the Loess Plateau, Northwest A&F University, Yangling, China

²Research Center of Soil and Water Conservation and Ecological Environment, Ministry of Education, Chinese Academy of Sciences, Yangling, China

³University of Chinese Academy of Sciences, Beijing, China

⁴CAS Center for Excellence in Quaternary Science and Global Change, Xi'an, China

⁵State Key Laboratory of Soil and Sustainable Agriculture, Institute of Soil Science, Chinese Academy of Sciences, Nanjing, China

⁶BioTechnology Institute, University of Minnesota, St. Paul, Minnesota, USA

⁷Department of Soil, Water, and Climate, University of Minnesota, St. Paul, Minnesota, USA

⁸Department of Forest Resources, University of Minnesota, St. Paul, Minnesota, USA

⁹Institute for Global Change Biology, University of Michigan, Ann Arbor, Michigan, USA

Correspondence

Xiaorong Wei, 26 Xinong Road, Yangling 712100, Shaanxi Province, China.
Email: weixr@nwsuaf.edu.cn;
xrwei78@163.com

Funding information

National Natural Science Foundation of China, Grant/Award Number: 41977068 and 41977105; programs from Chinese Academy of Sciences, China, Grant/Award Number: QYZDB-SSW-DQC039; Strategic Priority Research Program of the Chinese Academy of Sciences, China, Grant/Award Number: XDA23070202 and XDB40020000; US National Science Foundation (NSF) Biological Integration Institutes grant, Grant/Award Number: NSF-DBI-2021898

Abstract

Afforestation is an effective approach to rehabilitate degraded ecosystems, but often depletes deep soil moisture. Presently, it is not known how an afforestation-induced decrease in moisture affects soil microbial community and functionality, hindering our ability to understand the sustainability of the rehabilitated ecosystems. To address this issue, we examined the impacts of 20 years of afforestation on soil bacterial community, co-occurrence pattern, and functionalities along vertical profile (0–500 cm depth) in a semiarid region of China's Loess Plateau. We showed that the effects of afforestation with a deep-rooted legume tree on cropland were greater in deep than that of in top layers, resulting in decreased bacterial beta diversity, more responsive bacterial taxa and functional groups, increased homogeneous selection, and decreased network robustness in deep soils (120–500 cm). Organic carbon and nitrogen decomposition rates and multifunctionality also significantly decreased by afforestation, and microbial carbon limitation significantly increased in deep soils. Moreover, changes in microbial community and functionality in deep layer was largely related to changes in soil moisture. Such negative impacts on deep soils should be fully considered for assessing afforestation's eco-environment effects and for the sustainability of ecosystems because deep soils have important influence on forest ecosystems in semiarid and arid climates.

KEYWORDS

afforestation, deep soil layers, microbial diversity, microbial network, multifunctionality, semiarid region

1 | INTRODUCTION

In 2015, the United Nations initiated 17 Sustainable Development Goals (SDGs) for the sustainability of human societies and our natural resources. Thirteen of the 17 SDGs were directly or indirectly related to land development (Keesstra et al., 2016). Afforestation, converting degraded land to natural or secondary forests for the improvement of soil functions and the ecosystem services, plays a vital role in achieving land development related to the SDGs. Afforestation has been shown to significantly improve ecological and economical values of abandoned farmlands, including carbon sequestration, biomass production, hydrological regulation, climate regulation, and enhancing timber or food production (Knoke et al., 2014). For example, the Grain-for-Green Project initiated on China's Loess Plateau in 1999, one of the world's largest ecological restoration programs, has successfully rehabilitated severely degraded ecosystems (Wang et al., 2016). This large-scale program significantly reduced runoff and sediment discharge into the China's Yellow River and protected soil resources from loss, contributing significantly to the improvement of ecosystem services (Liu et al., 2020; Wang et al., 2016).

While the benefits of afforestation are well known, it can lead to increases in the interception of rainfall by plant canopies, as well as increases in evapotranspiration and root water uptake, resulting in the depletion of soil moisture (Oliveira et al., 2005; Wang et al., 2009), particularly in deep soils under arid and semiarid climates (Chen et al., 2008; Jia et al., 2017; Schlaepfer et al., 2017). It has been widely reported that restoration of vegetation on China's Loess Plateau accelerated soil water consumption by plants and formed a dry layer in the deep soils (Jia et al., 2020; Shao et al., 2016). Recent studies have shown that vegetation greening intensified soil drying in some semi-arid and arid areas of the world (Deng et al., 2020; Schlaepfer et al., 2017). Moreover, it has been suggested that afforestation-induced desiccation will ultimately threaten the health, sustainability, and services of restored ecosystems (Chen et al., 2008).

Soil microbes are essential for driving nutrient availability and biogeochemical cycles, supporting ecosystem evolution and functionality (Crowther et al., 2019; Delgado-Baquerizo et al., 2016). The diversity, composition, and association of soil microbes are sensitive to vegetation-related land-use changes. Afforestation has been shown to significantly increase soil microbial and functional diversity in upper soil horizons in various ecosystems (Han et al., 2019; Hu et al., 2019; Mukhopadhyay & Joy, 2010; Zhong et al., 2020). Afforestation usually increases microbial functionality (increased decomposition and decreased microbial nutrient limitation) in surface soils by directly or indirectly altering soil environments, such as nutrient availability, pH, porosity, soil moisture, and temperature (Cui et al., 2019; Yin et al., 2014; Zhong et al., 2020). However, our current understanding of the impact of afforestation on soil microbial processes has only focused on surface soils (0–40 cm depth), and most of the reported responses were largely dependent on nutrient changes following land-use changes. Given that soil microbes are sensitive to soil moisture (Barnard et al., 2013; Evans

& Wallenstein, 2014; Meisner et al., 2021), a better understanding of the linkages between afforestation-induced soil desiccation and microbial community and functionality in deep soils is particularly important for the sustainability of restored ecosystems.

In this study, we evaluated the impact of afforestation on microbial community structure and functionality in soils to a 500 cm depth in a semiarid region of China's Loess Plateau. We also determined how such changes are associated with soil nutrients and moisture changes. We hypothesized that the driving factors of afforestation impacts on the microbial community would shift with soil layers (top vs. deep layers) because this land-use change often increases nutrients in top soil, but decreases moisture in deep soils (Deng et al., 2017; Jia et al., 2020), while both factors determine microbial community in semiarid and arid climates (Chen et al., 2020; Malik et al., 2020). We also hypothesized that the diversity, stability, and functionality of the microbial community would increase in the top soils but decrease in deep soils after afforestation, due in large part to their dependence on soil nutrients and moisture (Chen et al., 2020; Wu et al., 2021). To test these hypotheses, we collected soil samples from a cropland and an adjacent forest of the nitrogen-fixing *Robinia* species that had been established on similar cropland 20 years ago due to the launch of the Grain for Green Project. We quantified bacterial diversity and composition by using 16S rRNA gene amplicon sequencing, and measured organic carbon and nitrogen mineralization and soil microbial nutrients metabolism limitation to assess microbial functionality, and also calculated soil multifunctionality. We also examined the relationships of soil microbial diversity, composition, robustness, and functionality to soil nutrients and moisture.

2 | MATERIALS AND METHODS

2.1 | Study site and soil sampling

This study was conducted in Dingbian county, Yulin City, Shaanxi province, China (108°4'E, 37°7'N). The study region has a semi-arid temperate continental monsoon climate, with a mean annual temperature of 7.9°C, mean annual precipitation of 312 mm, primarily occurring from July to September, and total annual potential evaporation of >2500 mm. This region is at an average elevation of 1605 m, and the site is dominated by Huangmian soil (a Calcaric Cambisol in the FAO classification), with a texture of sandy loam, developed on wind-deposited loessial parental material. Vegetation restoration activities, mainly converting cropland to woodland, were carried out in this region, as part of the Grain for Green Projects launched in 1999 (Cao et al., 2009).

In July 2020, we selected a typical sloping cropland site (ca. 10 ha) as the control and an adjacent forest site (ca. 10 ha) as the afforestation treatment to examine the impact(s) of afforestation on soil microbiota. Both sites had similar elevations and slope gradients (ca. 5 degrees) and had been previously subjected to similar farming practices. The cropland site was grassland before 1900s and was

converted to agricultural field to grow potato (*Solanum tuberosum* L.), fox-tail millet (*Setaria italica* [L.] P. Beauv.), and maize (*Zea mays* Linn.) after 1900s. The crops were planted in June and harvested in September. The site started to receive chemical fertilizers after 1980, with rates of 110–200 kg N ha⁻¹ as ammonium bicarbonate or urea and 0–80 kg P₂O₅ ha⁻¹ as calcium superphosphate or triple superphosphate among years. The cropland was abandoned after harvest in fall 2019, and did not receive any fertilizer after this time. Previous studies had shown that chemical fertilization has minimum effect on soil nutrients in cropland in the northern Loess Plateau (Yao et al., 2019), therefore this cropland could be used as control. The adjacent forest site had the same land use and management history with the cropland site until 1999, when the black locust (*Robinia pseudoacacia*) was planted on the previous farmland as part of the Grain for Green project. The forest site did not receive any fertilization and management measures since that time. The dominant species present was black locust, which in 2020 had an average height of 9.8 m and density of 2600 stems ha⁻¹.

On July 5, 2020, four replicate sampling plots (20 m × 20 m) were established in each of the cropland and forest sites. In each plot, five representative sampling points were randomly selected, and soils from these five points were combined into a composite sample for the plot. The sampling points in the forested land were located at least 1.0 m away from the stems of trees, and the organic and litter layers were removed from the soil surface prior to sampling. Soil samples from each plot were collected from the 0–20, 20–40, 40–80, 80–120, 120–180, 180–240, 240–300, 300–360, 360–420, and 420–500 cm depths using a soil auger (diameter, 5 cm). In total, 80 samples were collected (two land uses × four replicates × 10 depths). Soil samples were placed in an ice chest and transported to the laboratory, passed through a 2-mm sieve, and divided into three subsamples. One sample was stored at –80°C for the high-throughput DNA sequence analyses, one was used for the measurement of soil organic carbon and nitrogen mineralization, extracellular enzyme activity, available nitrogen and soil moisture, and the third was air-dried for the measurement of soil physicochemical properties.

2.2 | Soil physicochemical properties, extracellular enzyme activities, and potential microbial decomposition

Soil physicochemical properties were measured using standard methods as described by Qiu et al. (2021). Soil moisture was measured by oven-drying soils at 105°C to constant weight. Soil organic carbon (SOC) content was determined using the Walkley–Black method, and total nitrogen (TN) content was determined using the Kjeldahl method. Soil nitrate (NO₃⁻) and ammonium (NH₄⁺) concentrations were measured using an Auto-analyzer 3 (SEAL Analytical, Norderstedt, Germany) after extraction with 2 mol L⁻¹ KCl. Soil available phosphorus (OP) was determined by Olsen method. Soil pH was measured in a soil: water extract (1:2.5) with a pH meter (Mettler Toledo, Germany).

Activities of extracellular enzymes potentially involved in carbon, nitrogen, and phosphorous acquisition were measured by using a microplate-scale fluorometric method (Cui et al., 2019; Giacometti et al., 2014). The carbon-acquiring enzymes examined were β-1,4-glucosidase (BG) and β-D-cellobiohydrolase (CBH), the nitrogen-acquiring enzymes were β-1,4-N-acetylglucosaminidase (NAG) and L-leucine aminopeptidase (LAP), the phosphorous-acquiring enzyme was alkaline phosphatase (AP). The potential and relative microbial nutrient limitation was quantified using a vector analysis of soil enzymatic stoichiometry method by calculating vector length (relative carbon vs. nutrient limitation) and degree (relative phosphorous vs. nitrogen limitation) as follows (Moorhead et al., 2013):

$$\text{Vector length} = \sqrt{x^2 + y^2}$$

$$\text{Vector Degree} = \text{atan2}(y, x) \times 180 / \pi$$

where x represents the relative enzyme activities of carbon vs. nitrogen acquisition, i.e., (BG + CBH)/(BG + CBH + NAG + LAP); y represents the relative enzyme activities of carbon vs. phosphorous acquisition, i.e., (BG + CBH)/(BG + CBH + AP). Both x and y were calculated by the untransformed proportional enzyme activities.

Potential microbial decompositions (organic carbon and nitrogen mineralization) were determined by incubating 10 g soil samples at 25°C and 60% field moisture capacity in a 250 ml jar for 30 days in the dark (Wei et al., 2016). The amount of CO₂ released from soils after 1, 3, 7, 14, 21, 28 days of incubation was captured by 1 mol L⁻¹ NaOH and was measured by titration against 0.5 mol L⁻¹ HCl. Cumulative organic carbon mineralization (C_{min}, mg CO₂ kg⁻¹) was calculated by summing the total amount of CO₂ released from soils during the incubation period. Net nitrogen mineralization (N_{min}, mg kg⁻¹) was calculated by subtracting the concentrations of mineral nitrogen (NO₃⁻ + NH₄⁺) in soils before incubation from those after incubation. We also constructed the multifunctionality index related to nutrient cycling, including SOC, TN, C/N, OP, NH₄⁺, NO₃⁻, BG, CBH, LAP, NAG, AP, C_{min}, and N_{min}. These variables were the most commonly selected indicators for multifunctionality studies, and were considered to be key determinants of soil function in dryland ecosystems (Delgado-Baquerizo et al., 2013, 2016; Hu et al., 2021). The multifunctionality index based on these variables (z-scores) was calculated by using getStdAndMeanFunctions function in the multifunc package (<https://github.com/jebyrnes/multifunc>).

2.3 | High-throughput DNA sequencing and bioinformatics analysis

Total soil DNA was extracted using FastDNA Spin Kits (MP Biomedicals, Solon, OH, USA), following the manufacturer's instructions. The primers 341F (5'-CCTAYGGGRBGCASCAG-3') and 806R (5'-GGACTACHVGGGTWTCTAAT-3) (Muyzer et al., 1993; Yu et al., 2005) were used to amplify the V3–V4 regions of the 16S rRNA gene. All PCR reactions were carried out using 15 μl of Phusion®

High-Fidelity PCR Master Mix (New England Biolabs), 0.2 μ M of forward and reverse primers, and about 10 ng template DNA. The samples were amplified by the following conditions: initial denaturation at 98°C for 1 min, followed by 30 cycles of denaturation at 98°C for 10 s, annealing at 50 °C for 30s, extension at 72°C for 30s, and a final extension at 72°C for 5 min (Liang et al., 2020). Amplicons from triplicate reactions were pooled together for each sample and subjected to electrophoresis detection in a 2% (w/v) agarose gels. PCR products were purified using Qiagen Gel Extraction Kit (Qiagen, Germany). Sequencing libraries with sample index tags were generated using TruSeq® DNA PCR-Free Sample Preparation Kit (Illumina, USA) following manufacturer's recommendations. The library quality was assessed by the Qubit® 2.0 Fluorometer (Thermo Scientific) and Agilent Bioanalyzer 2100 system. Sequencing was performed on the Illumina NovaSeq platform to generate 250-bp paired-end reads at the Novogene Company, Beijing, China.

Sequences were trimmed, quality filtered, dereplicated, and generated amplicon sequence variants (ASVs) by using DADA2 program (Callahan et al., 2016) based on default settings in QIIME2-2020.11 pipeline (Bolyen et al., 2019). Amplicon reads of forward and reverse were trimmed to 220 and 220 bases, respectively. Sequences were taxonomically classified using the scikit-learn naive Bayesian classifier against the weighted SILVA 138 database. MAFFT and FastTree were used to align and construct the phylogenetic tree, respectively (Katoh & Frith, 2012; Price et al., 2010). The potential functional annotation and metabolic prediction were conducted by Tax4Fun2 package (<https://github.com/bwemheu/Tax4Fun2>). After singletons, chloroplast and mitochondrial sequences were removed, a total of 2,632,653 high-quality sequences (range 22,754–45,026; median 32,877 sequences per sample) were retained. Rarefaction curves indicated that the sequencing depth has reached saturation (Figure S1). All samples were rarefied to minimum sequences for downstream analysis.

2.4 | Statistical analyses

All statistical analyses were done using R environment (v4.0.5, <http://www.r-project.org/>). Our preliminary analysis showed that the response patterns of most measured parameters (soil nutrients, moisture, microbial diversity, composition, functionality, dominant phyla and families) to afforestation (forest vs. cropland) were markedly different between the 0–120 cm and 120–500 cm layers (Figures S2 and S3). However, although soil metrics varied with depth in the 0–120 cm layer, the responses of most parameters to afforestation were not significantly affected by sampling depth within 0–120 cm or 120–500 cm layer as suggested by the less significant interactions between afforestation and sampling depth in either layer (Table S1). Consequently, and hereafter, we grouped the soils at various depths into top (0–120 cm) and deep (120–500 cm) layers, rather than each sampling depth, to assess the differences in afforestation effects.

To examine the dissimilarities in bacterial communities among soil layers, principal coordinate analysis (PCoA) based on

Bray-Curtis distance, permutational multivariate analysis of variance (PERMANOVA), and homogeneity of multivariate dispersions (PERMDISP) were performed using the vegan package (<https://github.com/vegandevs/vegan>). The beta-diversity (Bray-Curtis dissimilarity) was partitioned into the abundance gradient (richness) and the balanced variation (turnover) using the bray.part function of the betapart package (<https://github.com/cran/betapart>), and its relationships to soil factors was evaluated by Mantel test. The relationships between community composition and soil properties were assessed using distance-based redundancy analysis (dbRDA) with Bray-Curtis dissimilarities, and individual effect of each soil factor was examined by rdacca.hp package (Lai et al., 2022).

Differential abundance analyses were done to examine the afforestation-responsive ASVs for each soil layer using the DESeq2 negative-binomial Wald test on non-rarefied reads (<https://github.com/mikelove/DESeq2>). The significance was evaluated at a false discovery rate (FDR)-corrected p value of $<.05$ (Benjamini & Hochberg, 1995). Phylogenetic distributions and relative abundance of the responsive taxa were constructed using ggtree package (<https://github.com/YuLab-SMU/ggtree>). Additionally, the Wilcoxon test was used to determine effects of afforestation on bacterial taxa of dominant phyla, orders, families, and genera as well as predicted metabolic functions. Heatmaps were used to display the relative abundance of taxa and their Spearman correlation with soil properties.

Null model analysis was used to evaluate the assembly processes of bacterial community (Stegen et al., 2012, 2013). Phylogenetic Mantel correlogram revealed a significant positive phylogenetic signal across short phylogenetic distances (Figure S4). In the model construction, β -nearest taxon index (β NTI) and the Bray-Curtis-based Raup-Crick (RC_{bray}) were calculated to quantify the relative importance of deterministic processes (e.g., variable selection and homogeneous selection) and stochastic processes (e.g., dispersal limitation, homogeneous dispersal and non-dominant). When $|\beta$ NTI| > 2 , the community turnover is governed by variable or homogeneous selection. When $|\beta$ NTI| < 2 and $|RC_{bray}| > 0.95$, the community turnover is governed by homogeneous dispersal or dispersal limitation, while $|\beta$ NTI| < 2 and $|RC_{bray}| < 0.95$ indicate the influence of the non-dominant process (Stegen et al., 2015; Tripathi et al., 2018). Additional Mantel tests were done to assess variations in community assembly processes after afforestation by evaluating the relationship between β NTI values and the Euclidean distance matrices of soil variables.

Co-occurrence network analyses were done based on samples from cropland and forest of top and deep layers. Taxa that accounted for more than half of samples in each of the four groups were used to calculate Spearman correlations coefficient, and P -values were adjusted by using the Benjamini and Hochberg FDR test for false discovery correction (Benjamini & Hochberg, 1995). Statistically robust correlations were identified when Spearman's $\rho > 0.7$ and the FDR-adjusted $p < .05$, and were then incorporated into subsequent network construction. Erdős-Rényi random networks (1000 iterations) in an equal size were constructed to compare with the real

network. Network topological parameters, including node number, edge, degree, betweenness centrality, closeness centrality, and eigenvector, were calculated using the igraph package (<https://github.com/igraph/igraph>). Network robustness was evaluated by natural connectivity (Fan et al., 2018; Mo et al., 2021; Peng & Wu, 2016) and cohesion index (Hernandez et al., 2021). Network with higher natural connectivity and absolute negative to positive cohesion ratio tends to be more stable (Hernandez et al., 2021; Mo et al., 2021).

Piecewise structural equation models (SEMs) were constructed to examine the direct and indirect effects of changes in soil nutrients, moisture, and bacterial community composition in both top and deep soils on microbial functions (organic carbon and nitrogen mineralization, microbial nutrients limitations, and multifunctionality) after afforestation. Shipley's d-separation test was used to examine whether any paths are missing from the model and the $p > .05$ indicated that no paths were missing and the model was a good fit (Shipley, 2009, 2013). We reported the standardized coefficient for each path from each component model, and Fisher's C statistic and AIC values of the overall model by using the piecewiseSEM package (<https://github.com/jslefche/piecewiseSEM>).

3 | RESULTS

3.1 | Response of soil properties to afforestation

Afforestation in this semiarid region resulted in the accumulation of nutrients in the soil from the top layer, but soil desiccation in the deep layer (Figure 1a-c and Figure S5). The SOC, TN, and C/N were significantly greater in forest than cropland in the top layer, but were similar in the deep layer. The concentration of NH_4^+ was increased by afforestation in both layers, and the increase was greater in top than in deep layers. The NO_3^- and moisture were significantly decreased by afforestation in deep layer, but were not affected in the top layer.

3.2 | Response of microbial diversity and composition to afforestation

The alpha diversity of the bacterial community was similar between cropland and restored forest in both the top and deep layers (Figure S6). Principal coordinate analysis showed that the bacterial community was clustered by afforestation (forest vs. cropland) and soil layers (top vs. deep). The effect of afforestation ($R^2 = 0.16$, $p < .001$) was greater than that of soil layer ($R^2 = 0.05$, $p < .001$) (Figure 1d).

The beta diversity (Bray-Curtis dissimilarity) index and variation (distance to centroid) of the bacterial community were similar between cropland and forest in the top layer, but significantly decreased by afforestation in deep layer (Figure 1e,f). The Mantel test showed that the bacterial composition in the top layer was influenced by carbon and nitrogen, while that in deep layer was

influenced by soil moisture (Figure S7; Table S2). For example, the slope of the relationship between Bray-Curtis dissimilarity and Euclidean distance of soil nutrients was greater in the top (slope: 0.003; $R^2 = 0.20$; $p < .001$) than deep layers (slope: 0.001; $R^2 = 0.06$; $p < .001$) (Figure S7a,c), while the slope of relationship between Bray-Curtis dissimilarity and Euclidean distance of soil moisture was greater in the deep layer (slope = 0.03, $R^2 = 0.38$, $p < .001$) than top layers (slope = 0.01, $R^2 < 0.01$, $p = .118$) (Figure S7b,d).

3.3 | Differences in taxon abundance and related key drivers

Afforestation significantly shifted the bacterial community in this semiarid soil. The number of afforestation-responsive taxa was smaller in the top (268) than the deep soil layer (714). In addition, the responsive taxa in top layer were more sensitive to soil nutrients, while that in deep layer were more sensitive to soil moisture following afforestation (Figure 2a,b). At the phylum level, the bacterial community comprised primarily of *Actinobacteriota* (42%), *Proteobacteria* (16%), *Acidobacteriota* (9%), *Gemmatimonadota* (8%), *Chlorolexi* (8%), and *Bacteroidota* (7%). The soils from forest had significantly greater relative abundances of *Actinobacteriota*, *Gemmatimonadota*, *Myxococcota*, and *Verrucomicrobiota*, but smaller abundances of *Bacteroidota*, *Firmicutes*, *Gal15*, and *Nitrospirota* than the soils from cropland. Most of these effects (except for the *Gemmatimonadota*) were greater in the deep than the top layer (Figure 2c,d). Moreover, the effects of afforestation on most bacterial taxa at order, family and genus levels were also greater in deep than top layer (Figure S8).

Results from both RDA and variation partition analysis showed that the variations in bacterial community at either ASV level or phylum, order, family, or genus level were all determined by afforestation and SOC and TN in the top layer, but by afforestation and soil moisture in the deep layer (Figure 3 and Figure S9). Therefore, this land-use change induced shifts in bacterial community structure were significantly related to the changes in soil nutrients for top soils, but related to the changes in moisture for deep soils.

3.4 | The deterministic and stochastic processes of microbial community

Homogeneous selection (59.4%–90.6%) contributed the largest fraction of bacterial assembly across the land uses and soil layers (Figure 4a). Afforestation had limited effects on bacterial assembly in the top layer, but increased homogeneous selection and decreased dispersal limitation in the deep layer (Figure 4a). Soil nutrients (i.e., SOC, TN, C/N, NO_3^-) and moisture were the best predictor of assembly processes (i.e., βNTI and RC_{bray}) of bacterial communities in the top and deep layers, respectively (Table S2). Specifically, there was a continuous transition from $\beta\text{NTI} < -2$ when the C/N in the top layer or moisture in deep layer was most similar between samples toward $-2 < \beta\text{NTI} < +2$ at intermediate differences, respectively

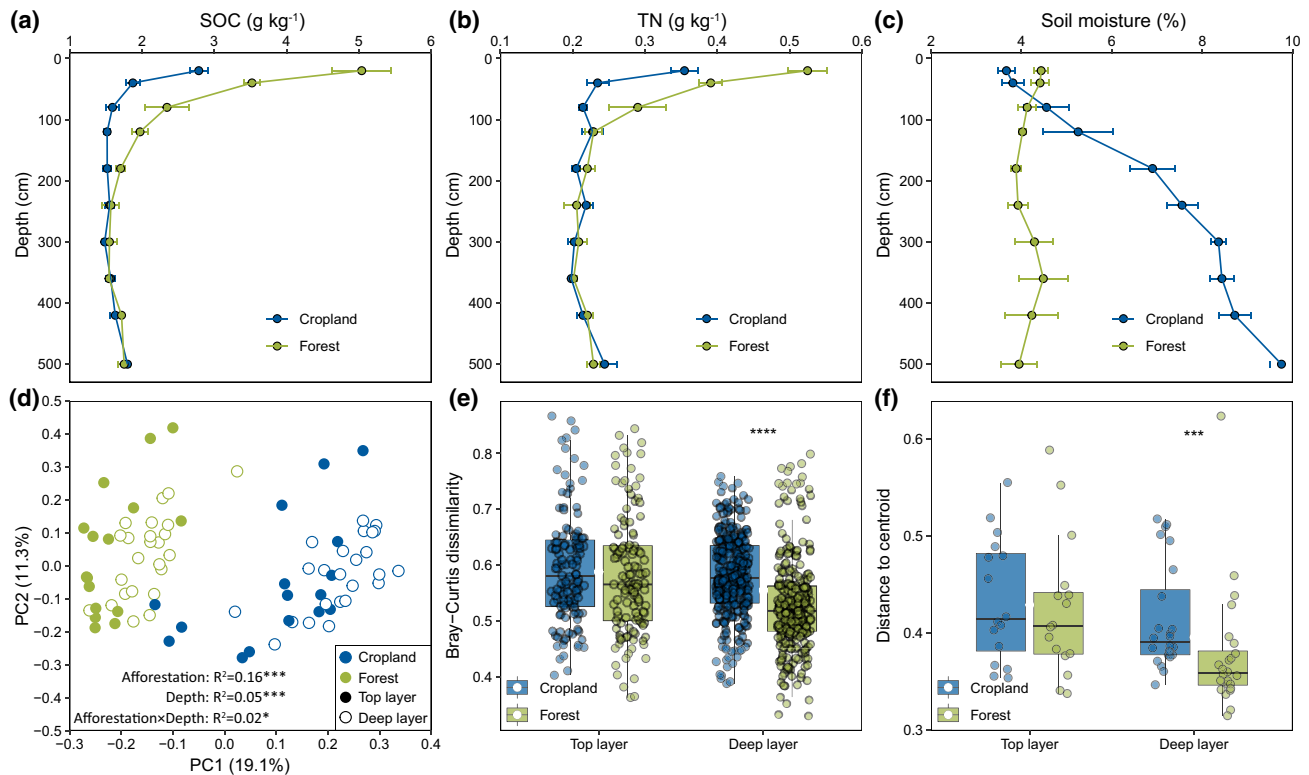


FIGURE 1 Variation in soil properties and bacterial communities induced by afforestation. (a–c) Variation in soil organic carbon (SOC), total nitrogen (TN), and moisture, respectively, along vertical profile of 0–500 cm depth after afforestation. (d) Principal coordinates analysis (PCoA) plot based on bray–Curtis distance. (e) Variation in beta diversity (bray–Curtis distance) in top (0–120 cm) and deep layers (120–500 cm) after afforestation. (f) Permutational analysis of multivariate dispersions (PERMDISP) showing dispersion among bacterial communities from different soil layers after afforestation. Box plots display the first (25%) and third (75%) quartiles, and median (bold line), and the maximum and minimum observed values. Asterisks denote significant differences based on the Wilcoxon test. * $p < .05$, ** $p < .01$, and *** $p < .001$. [Colour figure can be viewed at wileyonlinelibrary.com]

(Figure 4b,c). Hence, afforestation-induced nutrients change in the top layer and moisture changes in the deep layer likely contributed to the shift from homogeneous selection to stochasticity in the assembly of bacterial communities for both layers.

3.5 | Bacterial co-occurrence network

The degree of nodes in all the bacterial co-occurrence networks followed a power-law distribution (Figure S10), indicating a non-random distribution pattern. Afforestation had limited effects on the complexity of bacterial co-occurring network in the top layer, but increased the complexity in deep layer (Figure 5e–j). For the top layer, only the betweenness centrality and closeness centrality were significantly smaller in the forest than cropland, while for the deep layer, the examined parameters (degree, betweenness centrality, closeness centrality, and eigenvector) of the co-occurrence network were all significantly greater in the forest than the cropland soils (Figure 5g–j), indicating that the bacterial network in the deep layer was less robust in the forest than cropland. When examined for both layers, the effects of afforestation on bacterial co-occurrence network were closely associated with community composition and

responsive taxa. For instance, changes in node, edge, degree, and betweenness centrality after afforestation were significantly and positively correlated with Bray–Curtis dissimilarity of bacterial community (Figure S11). Moreover, the afforestation-responsive taxa were highly centralized and connected in the bacterial co-occurrence network, regardless of whether these were enriched or depleted taxa (Figure S12).

The natural connectivity was increased by afforestation in the top layer, but decreased in the deep layer (Figure 6a). Additionally, the negative/positive cohesion, a network property for predicting stability in co-occurrence networks, was also significantly decreased by afforestation in the deep layer (Figure 6b). Therefore, afforestation increased robustness of the bacterial co-occurring network in the top layer, but decreased the robustness in the deep layer.

3.6 | Linking environmental variables, bacterial community, and microbial functionalities

Forty-six potential metabolic functional groups of bacterial communities, analyzed via KEGG pathway (level 2), were predicted by the Tax4Fun2 package (Figure 7a,b). Afforestation resulted in the

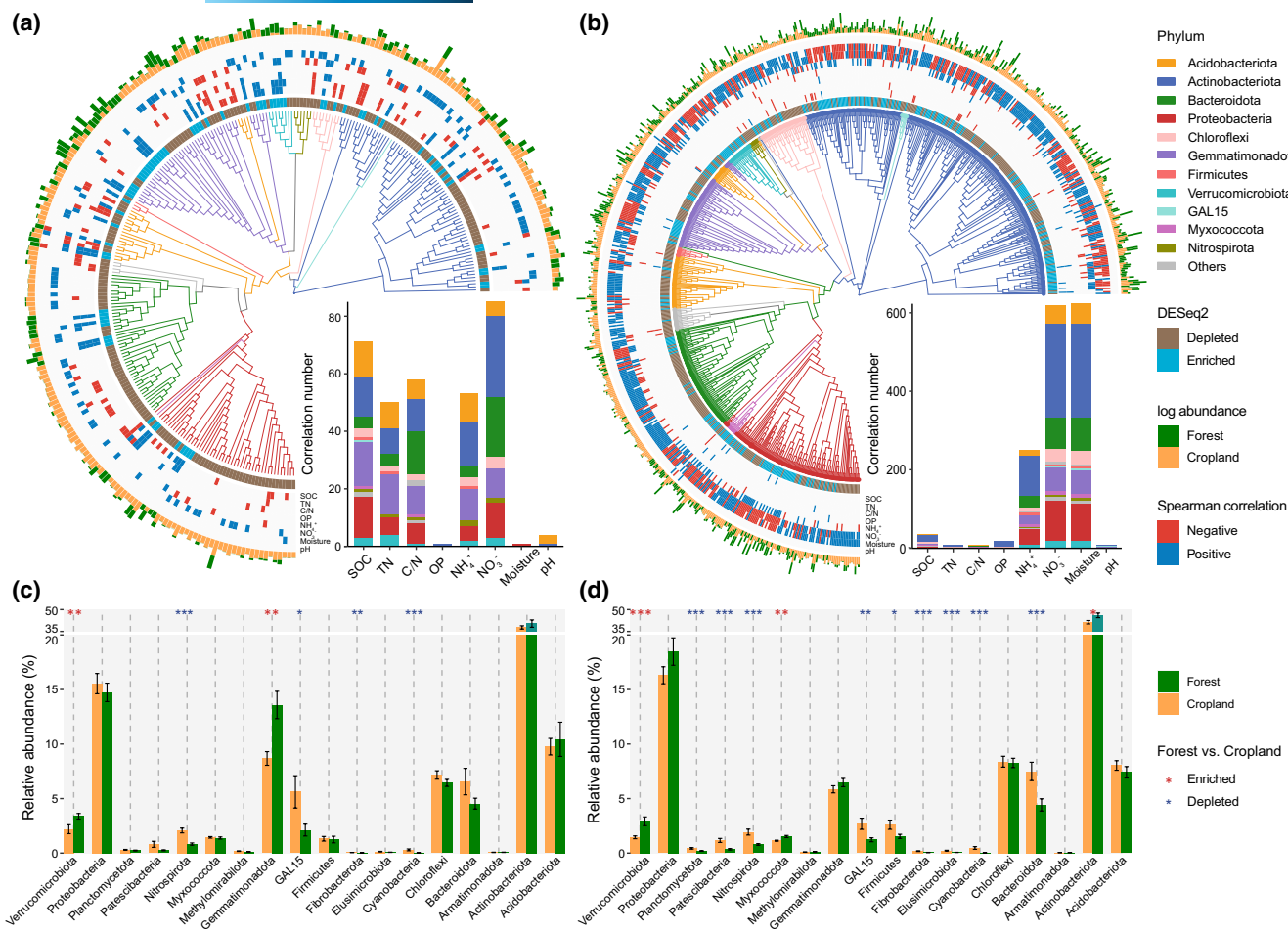


FIGURE 2 Responses of microbes to afforestation. Phylogeny of differentially abundant amplicon sequence variants (ASVs) between cropland and forest in top (0–120 cm) (a) and deep soil layer (120–150 cm) (b). These ASVs were identified using *DESeq2* package using cropland as a control. “Enriched” and “depleted” ASVs mean they were more and less abundant, respectively, in the forest than in the cropland. The outer rings show the log-transformed relative abundance of each ASV (the outermost ring) and their Spearman’s correlation to soil physicochemical properties (from inner to outer rings: SOC, TN, C/N, OP, NH₄⁺, NO₃⁻, moisture, and pH). Bar plots show the number of ASVs that were significantly correlated with specific soil physicochemical properties. The relative abundance of dominant phyla in cropland and forest in top (c) and deep soil layers (d), respectively. Significant changes in relative abundance of dominant phyla induced by afforestation in top and deep layers based on Wilcoxon test at $p < .05$ level. Legend: SOC, soil organic carbon; TN, soil total nitrogen; C/N, ratio of carbon to nitrogen; OP, available phosphorus; NH₄⁺, ammonium; NO₃⁻, nitrate; pH, soil pH; and moisture, soil moisture. Asterisks denote significant correlation. * $p < .05$, ** $p < .01$, and *** $p < .001$. [Colour figure can be viewed at wileyonlinelibrary.com]

decline in most bacterial metabolic functional groups. While 7 and 8 functional groups increased, 23 and 24 functional groups decreased in both top and deep layers, respectively (Figure 7c). For example, the relative abundances of groups related to carbohydrate metabolism, amino acid metabolism, and lipid metabolism decreased after afforestation, while those involved in xenobiotics biodegradation and metabolism increased. Moreover, most of these bacterial functional groups were significantly correlated with SOC and TN in the top layer, but were more influenced by soil moisture than nutrients in the deep layer (Figure 7d,e).

Effects of afforestation on microbial functionality also varied with soil layers. For the top layer, afforestation did not affect microbial decomposition, decreased metabolic limitation, and increased multifunctionality (Figure 8a). However, for the deep layer, afforestation significantly reduced decomposition of organic

carbon and nitrogen, increased microbial carbon limitation (vector length), but decreased microbial phosphorous limitation (vector angle) and multifunctionality (Figure 8a). The measured soil microbial functionalities were closely related to SOC, TN, and available N for the top layer (Figure S13a), but were closely related to SOC, available N, moisture, and microbial community for the deep layer, respectively (Figure S13b). Structural equation modeling showed that changes in microbial functionality in the top layer were mainly affected by afforestation-induced nutrients changes (Figure 8b), while these in deep layer were not only affected by nutrients changes, but also largely determined by soil moisture or its induced bacterial community composition changes (Figure 8c). Moreover, the impacts of nutrients on microbial functionality were smaller in the deep than in the top layer. Taken together, afforestation-induced soil desiccation can contribute to

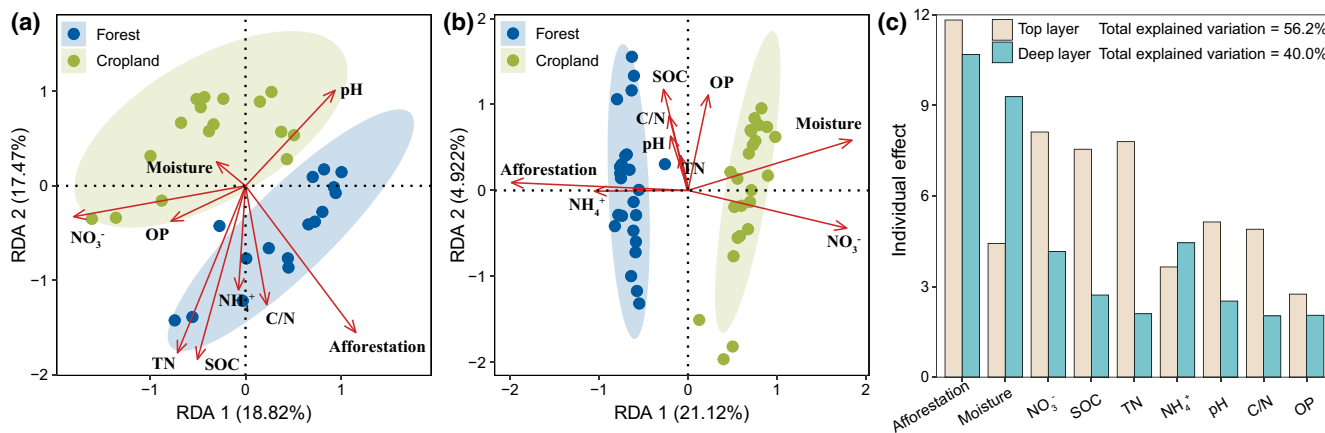


FIGURE 3 Variation in soil physicochemical properties induced by afforestation and their impacts on bacterial communities. Relationship between the community structures and soil properties in top (0–120 cm) (a) and deep soil layer (120–500 cm) (b), respectively, as assessed by distance-based redundancy analysis (dbRDA) based on bray–Curtis dissimilarity. The percentage in parentheses represents the variation explained by each axis. (c) Individual impact of each soil property is calculated based on rdacca.Hp package in top and deep layers. Legend: SOC, soil organic carbon; TN, soil total nitrogen; C/N, ratio of carbon to nitrogen; OP, available phosphorus; NH₄⁺, ammonium; NO₃⁻, nitrate; pH, soil pH; and moisture, soil moisture. [Colour figure can be viewed at wileyonlinelibrary.com]

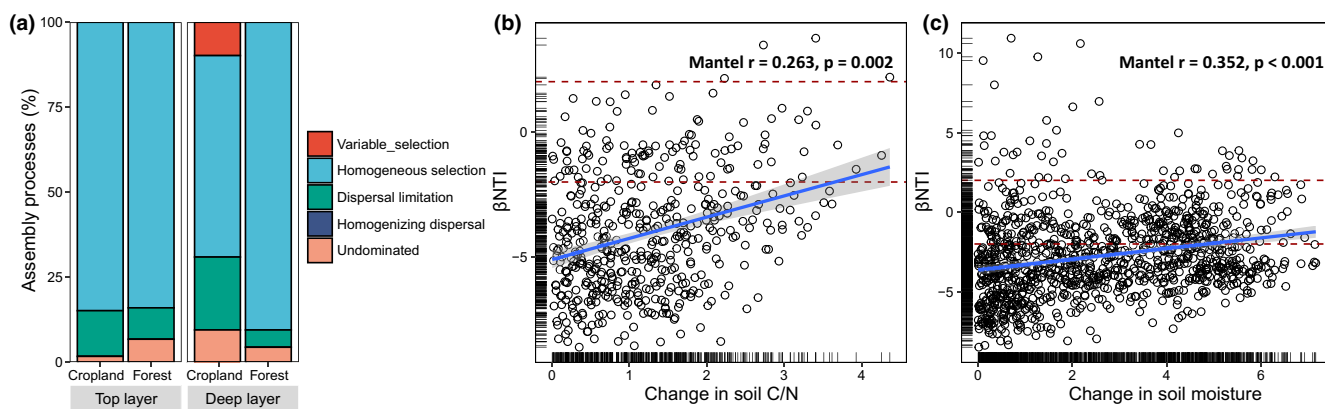


FIGURE 4 Relative influence of deterministic and stochastic assembly processes in shaping bacterial community after afforestation. (a) Contributions of ecological assembly processes governing bacterial community turnover across top and deep layers, respectively. Relationships of β -nearest taxon index (β NTI) to variations in soil C/N for the top soil layer (b) and moisture for the deep soil layer (c), respectively. Horizontal dashed red lines indicated the β NTI significance thresholds of +2 and -2. Dissimilarity distance matrix of soil properties was calculated based on Euclidean distances. Linear relationships shown in blue lines were evaluated by using the Mantel test. [Colour figure can be viewed at wileyonlinelibrary.com]

the decrease of microbial functionality in deep soils in this semi-arid region.

4 | DISCUSSION

4.1 | Afforestation resulted in desiccation in deep soil

In this study, we showed that converting cropland to legume forest resulted in the accumulation of SOC and nutrients in top soils, but decreased moisture in the deep soils (below 120 cm), consistent with previous observations in various climates (Jia et al., 2017; Laganier et al., 2010). The increase of SOC and nutrients in top

soils was mainly due to the accumulation of organic materials in the forest, which released SOC and nutrients into surface soils (Richter et al., 1999; Wei et al., 2012). The leaching of this added SOC and nutrients in deep soils (Davidson et al., 2011), the relatively lower moisture in deep soils may restrict the decomposition of root biomass because this process is largely dependent on soil moisture (Balogh et al., 2011). In related studies, the canopy interception, evapotranspiration, and root water uptake by deep-rooted trees, such as *Robinia pseudoacacia* in this study, was much more than rates found in cropland, and enhanced the depletion of deep soil water (Jia et al., 2017; Oliveira et al., 2005; Wang et al., 2012), contributing to the decrease of moisture in the deep soils. Our soil

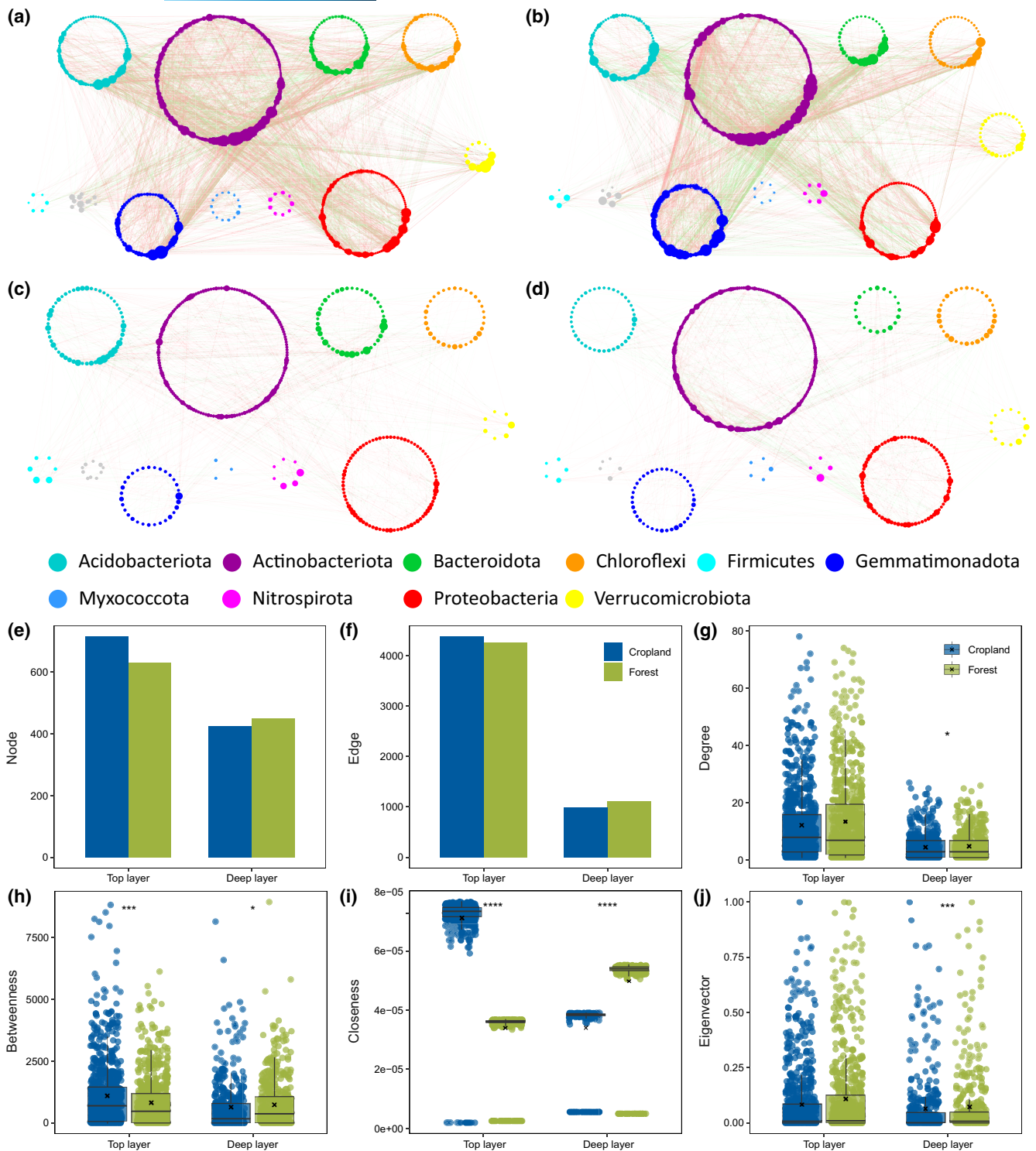


FIGURE 5 Bacterial co-occurrence networks for top soil layer in cropland (a), top soil layer in forest (b), deep soil layer in cropland (c), and deep soil layer in forest (d). Nodes in the network represent amplicon sequence variants (ASVs), and the color and size of each node show its phylum affiliation and the degree in the network. Red and green edges represent positive and negative interactions, respectively. Network properties, including node number (e), edge number (f), node connectedness (degree) (g), betweenness (h), closeness (i), and eigenvector (j). Asterisks denote significant differences based on the Wilcoxon test. * $p < .05$, ** $p < .01$ and, *** $p < .001$. [Colour figure can be viewed at wileyonlinelibrary.com]

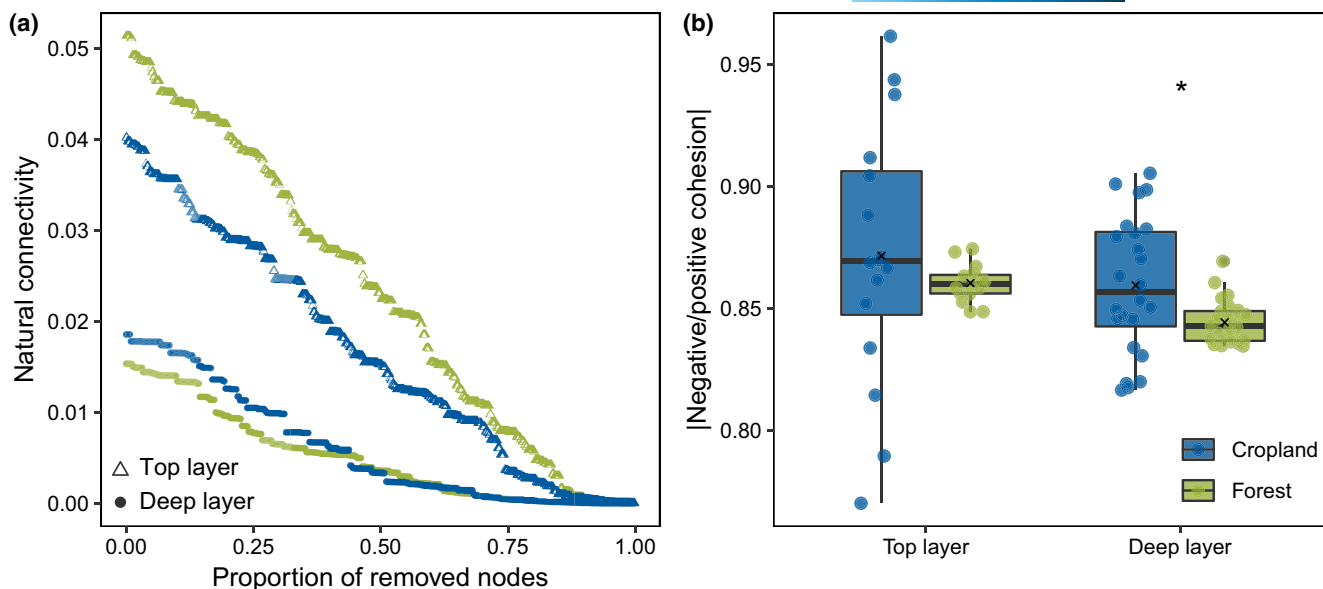


FIGURE 6 Bacterial co-occurrence network robustness, including natural connectivity (a) and absolute negative to positive cohesion ratio (b) affected by afforestation and soil depths. Asterisks denote significant differences based on the Wilcoxon test. * $p < .05$, ** $p < .01$ and *** $p < .001$. [Colour figure can be viewed at wileyonlinelibrary.com]

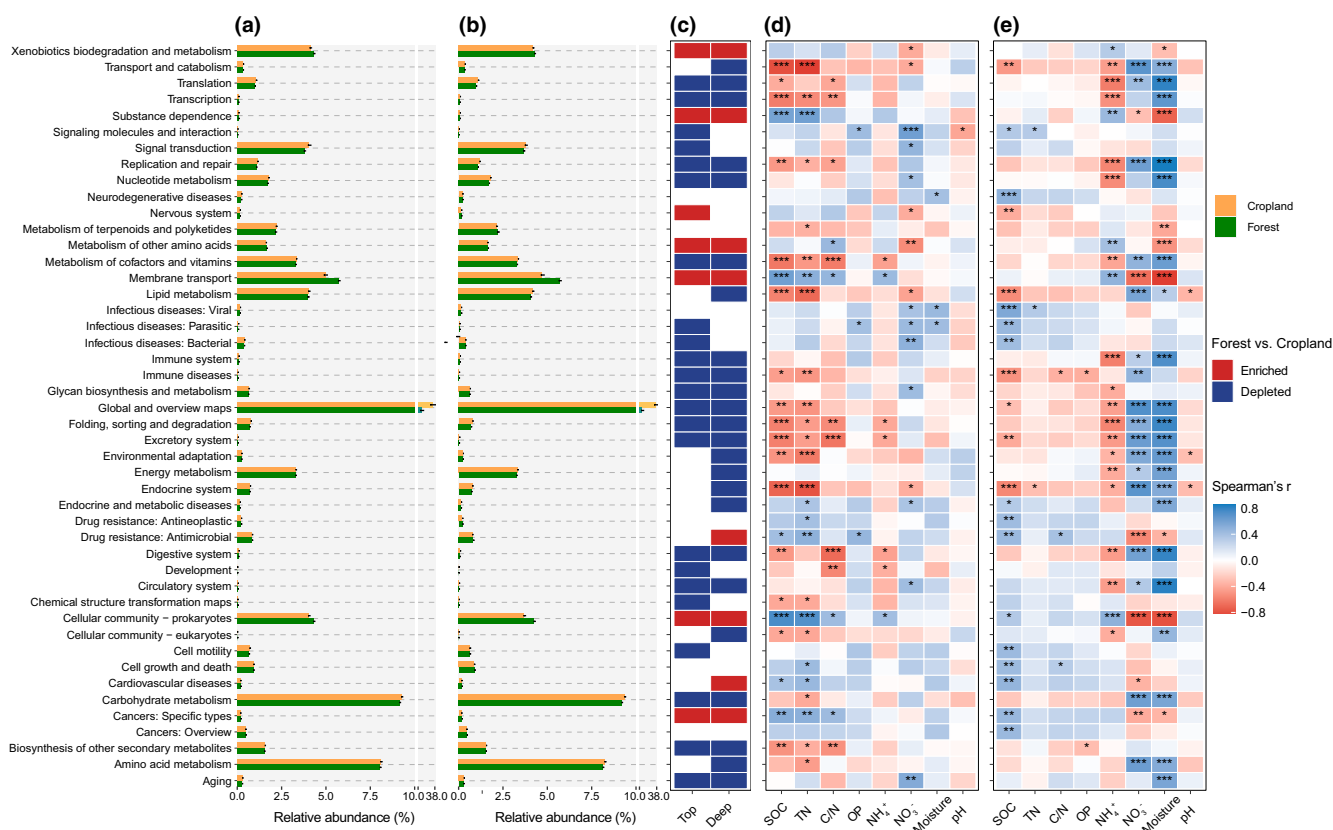


FIGURE 7 Variation in metabolic functions of bacterial communities after afforestation. The relative abundance of the 46 functions predicted by Tax4Fun2- KEGG pathway (level 2) in top (a) and deep soil layer (b), respectively. (c) Significant changes in relative abundance of predicted functions induced by afforestation in top and deep layers based on the Wilcoxon test at $p < .05$ level. The Spearman's correlation between predicted functions and soil physicochemical properties in top (d) and deep soil layer (e), respectively. Asterisks denote significant correlation. * $p < .05$, ** $p < .01$ and *** $p < .001$. [Colour figure can be viewed at wileyonlinelibrary.com]

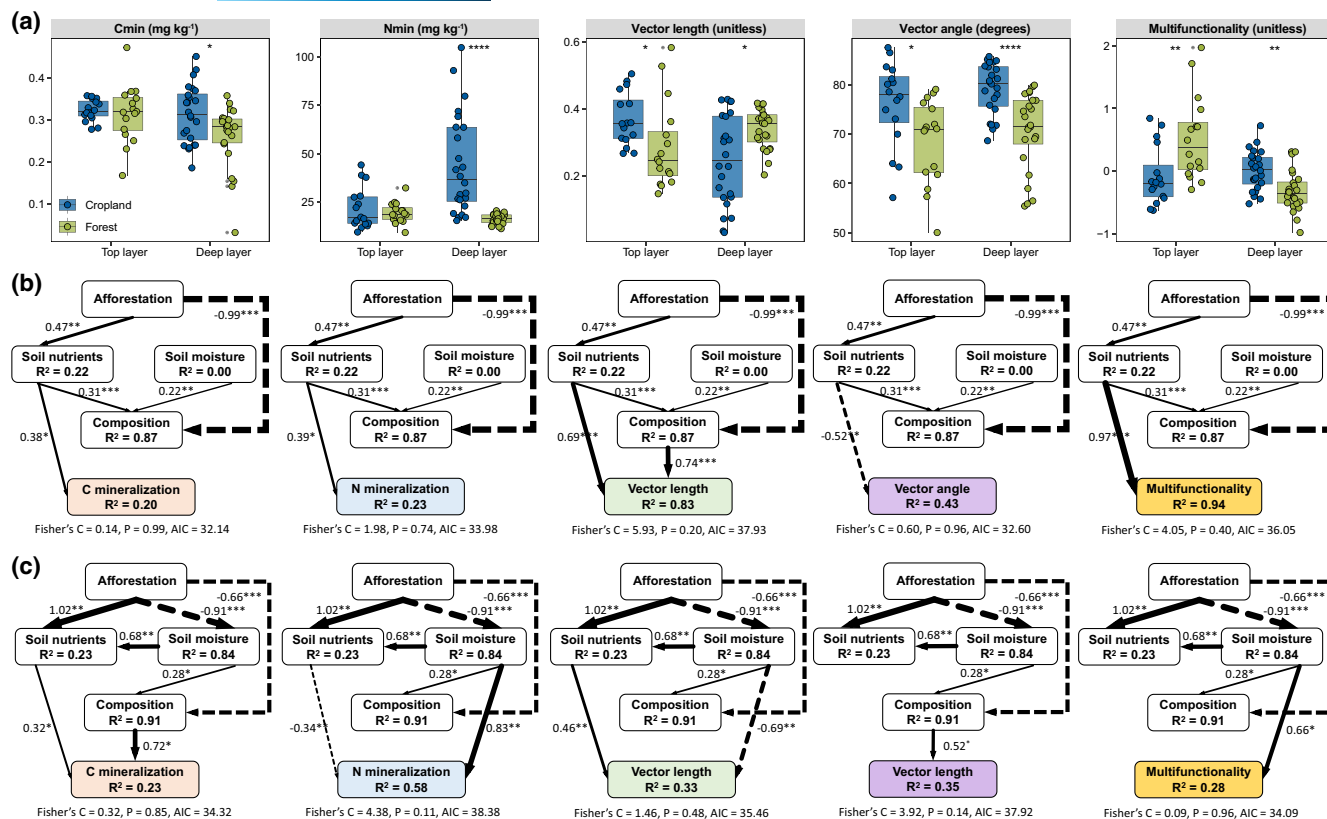


FIGURE 8 Soil microbial functionalities affected by afforestation and their driving factors. (a) Variation in soil microbial functionality (soil organic carbon and nitrogen mineralization, and vector length and vector angle) after afforestation in top and deep layers. Vector length represents relative C vs. nutrient limitation, and the vector angle denotes the relative P vs. N limitation. Asterisks denote significant differences based on Wilcoxon test at $p < .05$ level. Piecewise structural equation model (SEM) assessing the direct and indirect effects of afforestation, soil nutrient (the first axis of the principal component analysis based SOC, TN, OP, NH_4^+ and NO_3^-), moisture, and community composition (first axis of principal coordinates analysis) on five soil functions in top (b) and deep soil layers (c), respectively. Numbers adjacent to arrows show standardized path coefficients. Solid and dashed lines indicate positive and negative relationships, respectively. Non-significant pathways were not shown in the models. The R^2 values indicate the proportion of variance explained. Legend: SOC, soil organic carbon; TN, soil total nitrogen; C/N, ratio of carbon to nitrogen; OP, available phosphorus; NH_4^+ , ammonium; NO_3^- , nitrate. Asterisks denote significant differences based on the Wilcoxon test. * $p < .05$, ** $p < .01$, and *** $p < .001$ [Colour figure can be viewed at [wileyonlinelibrary.com](https://onlinelibrary.com)].

moisture results from a single soil sampling after 20 years of afforestation was highly consistent with the 10 years measurements of 0–4 m soil moisture under legume woodland on northern Loess Plateau (Jia et al., 2017).

4.2 | Soil moisture and nutrients influenced response of bacterial community to afforestation

We found that the changes in soil bacterial community in top layer were mainly related to soil nutrients, while that in deep soils was related to soil moisture. These results were expected because legumes typically increase soil N. The availability of SOC and nutrients can also shape microbial community composition in arid and semiarid climates, with higher nutrients availability inducing the growth of copiotrophs groups and inhibiting oligotrophic groups (Chen et al., 2020; Navarrete et al., 2015). In contrast, soil moisture can directly affect microbial physiological stress, growth, and metabolic activity

responses by changing osmotic pressure (Evans & Wallenstein, 2014; Kieft et al., 1987; Na et al., 2019; Schimel et al., 2007) and indirectly affect these parameters by changing resource/substrate availability (Na et al., 2019; Wang et al., 2018). Hence, the limitation of nutrients to microbes might be enhanced in dry conditions (Fuchslueger et al., 2014; Meisser et al., 2019).

In this study, we also show that afforestation increased the relative abundance of the phylum *Actinobacteriota* and taxa belonging to this phylum such as *MB-A2-108* and *Gaiella* in deep layer (Figure 2d and Figure S8c). This change was most likely related to a decrease in soil moisture given that the relative abundance of this taxon increases under soil moisture deficits (Banerjee et al., 2016; Naylor & Coleman-Derr, 2017; Ochoa-Hueso et al., 2018). Afforestation also resulted in a decrease in the relative abundance of the family *Nitrospriciaceae* (Figure S8b). The *Nitrospriciaceae* is more competitive in a low-nutrient environment (Frey et al., 2021; Schlatter et al., 2020) and has been found to be consistently enriched in deeper soil profiles (Schlatter et al., 2020; Upton et al., 2020). It has also been reported

that water stress induced by afforestation decreases N availability for soil microorganisms and inhibits the microbial metabolic activity (Na et al., 2019).

Our results showing a decrease in beta diversity in the deep layer by afforestation (Figure 1e) could be ascribed to the fact that the growth of deep-rooted trees reduced the niche heterogeneity by homogenizing resources (e.g., moisture, SOC, and nutrients) in deep soils (Figure 1a-c and Figure S2). The homogenized resource was found to decrease variation in beta diversity of soil bacterial communities (Jiao et al., 2018; Leibold & McPeck, 2006). Additionally, we found that the homogeneous enrichment of bacteria in deep soils contributed a large fraction to bacterial community assembly (Figure 4a), which will ultimately result in lower beta diversity (Stegen et al., 2015; Xu et al., 2021). These explanations were supported by the strong dependence of beta diversity in deep layer on soil moisture variation (Table S2) and by the significant correlation between Bray–Curtis dissimilarity and potential biotic interactions based on co-occurrence network observed in this study (Figure S11b) and previous studies (Wang et al., 2021; Xu et al., 2021).

4.3 | Afforestation shift bacterial co-occurrence network and its robustness

In support of our initial hypotheses, we found a decrease in the robustness of the bacterial co-occurring network in deep soils after afforestation. We ascribed this decrease to afforestation-induced soil desiccation, as drought usually decreases bacterial robustness due to their lower resistance to abiotic stress (de Vries et al., 2018). This explanation is consistent with our current understanding that environmental stress (i.e., drought etc.) decreases microbial co-occurrence network robustness (de Vries et al., 2018; Hernandez et al., 2021; Shi et al., 2020; Wu et al., 2021). Additionally, the low stability of the bacterial co-occurrence network could also be characterized by high connectivity (degree) and centrality (betweenness and eigenvector) (Figure 5g–j) (de Vries et al., 2018; Wu et al., 2021). In our current study, afforestation-responsive taxa were highly centralized and connected, regardless of whether these were enriched or depleted taxa (Figure S12). This suggested that these taxa might drive the changes in the bacterial co-occurrence network (de Vries et al., 2018) and its robustness after afforestation. Such responsive taxa in the top layer were sensitive to nutrients, while those in the deep layer were more sensitive to moisture (Figure 2a,b), providing an explanation for the divergent response of microbial robustness in top and deep layers after afforestation. In contrast, the afforestation-induced increase in the robustness of the bacterial co-occurring network in top soils was likely due to the accumulation of organic material, which supply SOC and nutrients for the microbial activities (Fan et al., 2018). Additionally, soil drought stress in top soils can be alleviated to some degree by rainfall even in semi-arid and arid regions, and thus had minimum effects on microbial robustness in the top layer. Taken together, our results showed that

soil desiccation in deep layers contributed to the decreased robustness of bacterial co-occurring networks, while increases of soil SOC and nutrients in top soils contributed to increased robustness after afforestation.

4.4 | Decreased microbial functionality in deep soils after afforestation

In this study, afforestation decreased the relative abundances of functional groups related to carbohydrate metabolism, amino acid metabolism, and lipid metabolism, probably due to the enhanced soil drought by these deep-root trees as such functional groups are sensitive to water stress (Bromke, 2013; Chen et al., 2012; Corrigan et al., 2015). However, afforestation increased the relative abundances of groups involved in xenobiotics biodegradation and metabolism, likely due to the input of organic materials from forest. We also found that afforestation in cropland increased soil microbial functionality in top soils, but resulted in a decrease in deep soils based on the measured values (Figure 8a), primarily because soil microbes were more limited by soil water conditions in such microclimates (Cui et al., 2019; Leizeaga et al., 2020). For the top soils, the increase in nutrients and seasonal rainfall may alleviate the restriction of soil water on soil bacterial community structure and function. In contrast, for the deep soils, the decrease in soil moisture can cause drought stress to microbes and limit the availability of nutrients to bacteria by directly restraining the bacterial dispersion within physically protected soil pores (Giannetta et al., 2018). Additionally, a decrease in soil moisture resulted in disconnected resource islands, and thus created more severe carbon and nutrient limitations for soil microorganisms, compared with the environments that were not limited by water (Jansson & Hofmockel, 2020; Schimel, 2018). Therefore, in this semi-arid region, effects of afforestation-induced soil desiccation on soil microbial communities in deep soils were greater than those of nutrient enrichment in top soils (despite the N-fixation habit of the forest species).

5 | IMPLICATIONS

In the current study, the relationships between soil bacterial community and soil nutrients and moisture after 20-year afforestation on cropland were examined with the same soil at the same site. This experimental system allowed exclusion of soil texture and climate impacts on soil microbiota. Our results showed that the driving factor(s) for the changes in soil microbial community induced by afforestation shifted with soil layers in this semiarid region. Such shifts should be carefully considered because the soils in most arid and semiarid climates have depths of more than 1 m (many are tens of meters) (Jia et al., 2020; Plaza et al., 2018). It was previously postulated that microbes in deep soils (deeper than 100 cm) are

rarely affected by environmental factors (e.g., temperature, precipitation, land surface disturbance) (Fierer et al., 2003), especially in arid and semiarid regions of the world. This hypothesis may not be always true, and results we present here showed that afforestation resulted in a decrease in soil moisture, and a significant shift in bacterial community structure and functionality in deeper soils (500 cm). Consequently, land-use changes may have a greater impact than the environments on deep soil microbiota. Additionally, our results that afforestation had significant negative effects on microbial community structure and functionality in deep soils further suggested that current assessment focusing only on the top layer may underestimate effects of afforestation on ecosystem functionality and services.

It is well known that soil moisture and nutrient availability in deep layers are essential for the growth of deep-rooted plants, particularly in semiarid and arid regions where the plant growth depends more on deep soils moisture rather than rainfall water (Chen et al., 2008; Li et al., 2021; McGulley et al., 2004; Yang et al., 2012). Additionally, the drought-induced forest die-off observed in many regions (Goulden & Bales, 2019; Peng et al., 2011) is assumed to be closely related to soil drought. For example, it has been reported that multi-year deep soil drought in 2012–2015 drought led to California forest die-off (Goulden & Bales, 2019). However, here we demonstrated that afforestation-induced desiccation in deep soils decreased microbial functionality. Given that microbes play essential roles in increasing nutrient availability and water accessibility to roots (Jiao et al., 2018; Stewart et al., 2017), this result suggests that the degradation (i.e., die-off and/or decrease in functionality) of rehabilitated or natural forest in many semiarid regions (Chen et al., 2015; Fu et al., 2017; Goulden & Bales, 2019; Peng et al., 2011; Wang et al., 2008) might not only be due to the reduction of soil moisture, but also to the drought-induced microbial function loss in deep soils. Consequently, converting cropland to deep-rooted woodland for the sustainability of ecosystems should be carefully considered in arid and semiarid regions.

AUTHOR CONTRIBUTIONS

X.W. conceived this project. X.W. and W.K. processed the soil samples and collected data. W.K. conducted the bioinformatics analyses. L.Q., W.K., and X.W. wrote the first draft of the manuscript and Y.W., M.S., Q.Z., M.J.S., S.I., P.B.R., G.W., S.J., L.Q., and L.L. contributed to subsequent revisions. All authors contributed to the final written product.

ACKNOWLEDGMENTS

This study was supported, in part, by the Strategic Priority Research Program of the Chinese Academy of Sciences (XDA23070202 and XDB40020000), the National Natural Science Foundation of China (41977068 and 41977105), programs from Chinese Academy of Sciences (QYZDB-SSW-DQC039), and the US National Science Foundation (NSF) Biological Integration Institutes grant (NSF-DBI-2021898, to P.B.R.).

CONFLICT OF INTEREST

The authors declare no competing interests.

DATA AVAILABILITY STATEMENT

Sequencing data are available in the NCBI Sequence Read Archive repository under the accession number PRJNA778306. The other data that support the findings of this study are available in Dryad at <https://doi.org/10.5061/dryad.7sqv9s4vn>.

ORCID

Weibo Kong  <https://orcid.org/0000-0003-1309-5072>

Xiaorong Wei  <https://orcid.org/0000-0002-0359-0339>

Yonghong Wu  <https://orcid.org/0000-0002-2985-219X>

Peter B. Reich  <https://orcid.org/0000-0003-4424-662X>

REFERENCES

- Balogh, J., Pintér, K., Fóti, S., Cserhalmi, D., Papp, M., & Nagy, Z. (2011). Dependence of soil respiration on soil moisture, clay content, soil organic matter, and CO₂ uptake in dry grasslands. *Soil Biology and Biochemistry*, 43, 1006–1013. <https://doi.org/10.1016/j.soilbio.2011.01.017>
- Banerjee, S., Helgason, B., Wang, L., Winsley, T., Ferrari, B. C., & Siciliano, S. D. (2016). Legacy effects of soil moisture on microbial community structure and N₂O emissions. *Soil Biology and Biochemistry*, 95, 40–50. <https://doi.org/10.1016/j.soilbio.2015.12.004>
- Barnard, R. L., Osborne, C. A., & Firestone, M. K. (2013). Responses of soil bacterial and fungal communities to extreme desiccation and rewetting. *The ISME Journal*, 7, 2229–2241. <https://doi.org/10.1038/ismej.2013.104>
- Benjamini, Y., & Hochberg, Y. (1995). Controlling the false discovery rate: A practical and powerful approach to multiple testing. *Journal of the Royal Statistical Society: Series B (Methodological)*, 57, 289–300. <https://doi.org/10.1111/j.2517-6161.1995.tb02031.x>
- Bolyen, E., Rideout, J. R., Dillon, M. R., Bokulich, N. A., Abnet, C. C., Al-Ghalith, G. A., Alexander, H., Alm, E. J., Arumugam, M., Asnicar, F., Bai, Y., Bisanz, J. E., Bittinger, K., Brejnrod, A., Brislawn, C. J., Brown, C. T., Callahan, B. J., Caraballo-Rodriguez, A. M., Chase, J., ... Caporaso, J. G. (2019). Reproducible, interactive, scalable and extensible microbiome data science using QIIME 2. *Nature Biotechnology*, 37, 852–857. <https://doi.org/10.1038/s41587-019-0209-9>
- Bromke, M. A. (2013). Amino acid biosynthesis pathways in diatoms. *Metabolites*, 3, 294–311. <https://doi.org/10.3390/metabo3020294>
- Callahan, B. J., McMurdie, P. J., Rosen, M. J., Han, A. W., Johnson, A. J., & Holmes, S. P. (2016). DADA2: High-resolution sample inference from Illumina amplicon data. *Nature Methods*, 13, 581–583. <https://doi.org/10.1038/nmeth.3869>
- Cao, S., Chen, L., & Yu, X. (2009). Impact of China's grain for green project on the landscape of vulnerable arid and semi-arid agricultural regions: A case study in northern Shaanxi Province. *Journal of Applied Ecology*, 46, 536–543. <https://doi.org/10.1111/j.1365-2664.2008.01605.x>
- Chen, H., Shao, M., & Li, Y. (2008). Soil desiccation in the loess plateau of China. *Geoderma*, 143, 91–100. <https://doi.org/10.1016/j.geoderma.2007.10.013>
- Chen, L., Yang, Y., Deng, S., Xu, Y., Wang, G., & Liu, Y. (2012). The response of carbohydrate metabolism to the fluctuation of relative humidity (RH) in the desert soil cyanobacterium *Phormidium tenue*. *European Journal of Soil Biology*, 48, 11–16. <https://doi.org/10.1016/j.ejsobi.2011.10.002>
- Chen, Y., Neilson, J. W., Kushwaha, P., Maier, R. M., & Barberan, A. (2020). Life-history strategies of soil microbial communities in

- an arid ecosystem. *The ISME Journal*, 15, 649–657. <https://doi.org/10.1038/s41396-020-00803-y>
- Chen, Y., Wang, K., Lin, Y., Shi, W., Song, Y., & He, X. (2015). Balancing green and grain trade. *Nature Geoscience*, 8, 739–741. <https://doi.org/10.1038/ngeo2544>
- Corrigan, R. M., Bowman, L., Willis, A. R., Kaefer, V., & Grundling, A. (2015). Crosstalk between two nucleotide-signaling pathways in *Staphylococcus aureus*. *Journal of Biological Chemistry*, 290, 5826–5839. <https://doi.org/10.1074/jbc.M114.598300>
- Crowther, T. W., van den Hoogen, J., Wan, J., Mayes, M. A., Keiser, A. D., Mo, L., Averill, C., & Maynard, D. S. (2019). The global soil community and its influence on biogeochemistry. *Science*, 365, 772. <https://doi.org/10.1126/science.aav0550>
- Cui, Y., Fang, L., Guo, X., Han, F., Ju, W., Ye, L., Wang, X., Tan, W., & Zhang, X. (2019). Natural grassland as the optimal pattern of vegetation restoration in arid and semi-arid regions: Evidence from nutrient limitation of soil microbes. *Science of the Total Environment*, 648, 388–397. <https://doi.org/10.1016/j.scitotenv.2018.08.173>
- Davidson, E., Lefebvre, P. A., Brando, P. M., Ray, D. M., Trumbore, S. E., Solorzano, L. A., Ferreira, J. N., Bustamante, M., & Nepstad, D. C. (2011). Carbon inputs and water uptake in deep soils of an eastern Amazon forest. *Forest Science*, 57, 51–58. <https://doi.org/10.1093/forestscience/57.1.51>
- de Vries, F. T., Griffiths, R. I., Bailey, M., Craig, H., Girlanda, M., Gweon, H. S., Hallin, S., Kaisermann, A., Keith, A. M., Kretzschmar, M., Lemanceau, P., Lumini, E., Mason, K. E., Oliver, A., Ostle, N., Prosser, J. I., Thion, C., Thomson, B., & Bardgett, R. D. (2018). Soil bacterial networks are less stable under drought than fungal networks. *Nature Communications*, 9, 3033. <https://doi.org/10.1038/s41467-018-05516-7>
- Delgado-Baquerizo, M., Maestre, F. T., Gallardo, A., Bowker, M. A., Wallenstein, M. D., Quero, J. L., Ochoa, V., Gozalo, B., Garcia-Gomez, M., Soliveres, S., Garcia-Palacios, P., Berdugo, M., Valencia, E., Escolar, C., Arredondo, T., Barraza-Zepeda, C., Bran, D., Carreira, J. A., Chaieb, M., ... Zaady, E. (2013). Decoupling of soil nutrient cycles as a function of aridity in global drylands. *Nature*, 502, 672–676. <https://doi.org/10.1038/nature12670>
- Delgado-Baquerizo, M., Maestre, F. T., Reich, P. B., Jeffries, T. C., Gaitan, J. J., Encinar, D., Berdugo, M., Campbell, C. D., & Singh, B. K. (2016). Microbial diversity drives multifunctionality in terrestrial ecosystems. *Nature Communications*, 7, 10541. <https://doi.org/10.1038/ncomms10541>
- Deng, L., Han, Q., Zhang, C., Tang, Z., & Shangguan, Z. (2017). Above-ground and below-ground ecosystem biomass accumulation and carbon sequestration with *Caragana korshinskii* Kom plantation development. *Land Degradation and Development*, 28, 906–917. <https://doi.org/10.1002/ldr.2642>
- Deng, Y., Wang, S., Bai, X., Luo, G., Wu, L., Chen, F., Wang, J., Li, C., Yang, Y., Hu, Z., Tian, S., & Lu, Q. (2020). Vegetation greening intensified soil drying in some semi-arid and arid areas of the world. *Agricultural and Forest Meteorology*, 292–293, 108103. <https://doi.org/10.1016/j.agrformet.2020.108103>
- Evans, S. E., & Wallenstein, M. D. (2014). Climate change alters ecological strategies of soil bacteria. *Ecology Letters*, 17, 155–164. <https://doi.org/10.1111/ele.12206>
- Fan, K., Weisenhorn, P., Gilbert, J. A., & Chu, H. (2018). Wheat rhizosphere harbors a less complex and more stable microbial co-occurrence pattern than bulk soil. *Soil Biology & Biochemistry*, 125, 251–260. <https://doi.org/10.1016/j.soilbio.2018.07.022>
- Fierer, N., Schimel, J. P., & Holden, P. A. (2003). Variations in microbial community composition through two soil depth profiles. *Soil Biology and Biochemistry*, 35, 167–176. [https://doi.org/10.1016/S0038-0717\(02\)00251-1](https://doi.org/10.1016/S0038-0717(02)00251-1)
- Frey, B., Walthert, L., Perez-Mon, C., Stierli, B., Köchli, R., Dharmarajah, A., & Brunner, I. (2021). Deep soil layers of drought-exposed forests harbor poorly known bacterial and fungal communities. *Frontiers in Microbiology*, 12, 674160. <https://doi.org/10.3389/fmicb.2021.674160>
- Fu, B., Wang, S., Liu, Y., Liu, J., Liang, W., & Miao, C. (2017). Hydrogeomorphic ecosystem responses to natural and anthropogenic changes in the loess plateau of China. *Annual Review of Earth and Planetary Sciences*, 45, 223–243. <https://doi.org/10.1146/annurev-earth-063016-020552>
- Fuchslueger, L., Bahn, M., Fritz, K., Hasibeder, R., & Richter, A. (2014). Experimental drought reduces the transfer of recently fixed plant carbon to soil microbes and alters the bacterial community composition in a mountain meadow. *New Phytologist*, 201, 916–927. <https://doi.org/10.1111/nph.12569>
- Giacometti, C., Cavani, L., Baldoni, G., Ciavatta, C., Marzadori, C., & Kandeler, E. (2014). Microplate-scale fluorometric soil enzyme assays as tools to assess soil quality in a long-term agricultural field experiment. *Applied Soil Ecology*, 75, 80–85. <https://doi.org/10.1016/j.apsoil.2013.10.009>
- Giannetta, B., Plaza, C., Vischetti, C., Cotrufo, M. F., & Zaccaro, C. (2018). Distribution and thermal stability of physically and chemically protected organic matter fractions in soils across different ecosystems. *Biology and Fertility of Soils*, 54, 671–681. <https://doi.org/10.1007/s00374-018-1290-9>
- Goulden, M. L., & Bales, R. C. (2019). California forest die-off linked to multi-year deep soil drying in 2012–2015 drought. *Nature Geoscience*, 12, 632–637. <https://doi.org/10.1038/s41561-019-0388-5>
- Han, X., Ren, C., Li, B., Yan, S., Fu, S., Gao, D., Zhao, F., Deng, J., & Yang, G. (2019). Growing seasonal characteristics of soil and plants control the temporal patterns of bacterial communities following afforestation. *Catena*, 178, 288–297. <https://doi.org/10.1016/j.catena.2019.03.021>
- Hernandez, D. J., David, A. S., Menges, E. S., Searcy, C. A., & Afkhami, M. E. (2021). Environmental stress destabilizes microbial networks. *The ISME Journal*, 15, 1722–1734. <https://doi.org/10.1038/s41396-020-00882-x>
- Hu, W., Ran, J., Dong, L., Du, Q., Ji, M., Yao, S., Sun, Y., Gong, C., Hou, Q., Gong, H., Chen, R., Lu, J., Xie, S., Wang, Z., Huang, H., Li, X., Xiong, J., Xia, R., Wei, M., ... Deng, J. (2021). Aridity-driven shift in biodiversity-soil multifunctionality relationships. *Nature Communications*, 12, 5350. <https://doi.org/10.1038/s41467-021-25641-0>
- Hu, Y., Zhang, Z., Huang, L., Qi, Q., Liu, L., Zhao, Y., Wang, Z., Zhou, H., Lv, X., Mao, Z., Yang, Y., Zhou, J., & Kardol, P. (2019). Shifts in soil microbial community functional gene structure across a 61-year desert revegetation chronosequence. *Geoderma*, 347, 126–134. <https://doi.org/10.1016/j.geoderma.2019.03.046>
- Jansson, J. K., & Hofmockel, K. S. (2020). Soil microbiomes and climate change. *Nature Reviews Microbiology*, 18, 35–46. <https://doi.org/10.1038/s41579-019-0265-7>
- Jia, X., Shao, M., Wei, X., Zhu, Y., Wang, Y., & Hu, W. (2020). Policy development for sustainable soil water use on China's loess plateau. *Science Bulletin*, 65, 2053–2056. <https://doi.org/10.1016/j.scib.2020.09.006>
- Jia, X., Shao, M., Zhu, Y., & Luo, Y. (2017). Soil moisture decline due to afforestation across the loess plateau, China. *Journal of Hydrology*, 546, 113–122. <https://doi.org/10.1016/j.jhydrol.2017.01.011>
- Jiao, S., Chen, W., Wang, J., Du, N., Li, Q., & Wei, G. (2018). Soil microbiomes with distinct assemblies through vertical soil profiles drive the cycling of multiple nutrients in reforested ecosystems. *Microbiome*, 6, 146. <https://doi.org/10.1186/s40168-018-0526-0>
- Katoh, K., & Frith, M. C. (2012). Adding unaligned sequences into an existing alignment using MAFFT and LAST. *Bioinformatics*, 28, 3144–3146. <https://doi.org/10.1093/bioinformatics/bts578>
- Keesstra, S. D., Bouma, J., Wallinga, J., Tittoneil, P., Smith, P., Cerdà, A., Montanarella, L., Quinton, J. N., Pachepsky, Y., van der Putten, W. H., Bardgett, R. D., Moolenaar, S., Mol, G., Jansen, B., & Fresco, L. O. (2016). The significance of soils and soil science towards realization of the United Nations sustainable development goals. *The Soil*, 2, 111–128. <https://doi.org/10.5194/soil-2-111-2016>

- Kieft, T. L., Soroker, E., & Firestone, M. K. (1987). Microbial biomass response to a rapid increase in water potential when dry soil is wetted. *Soil Biology and Biochemistry*, *19*, 119–126. [https://doi.org/10.1016/0038-0717\(87\)90070-8](https://doi.org/10.1016/0038-0717(87)90070-8)
- Knoke, T., Bendix, J., Pohle, P., Hamer, U., Hildebrandt, P., Roos, K., Gerique, A., Sandoval, M. L., Breuer, L., Tischer, A., Silva, B., Calvas, B., Aguirre, N., Castro, L. M., Windhorst, D., Weber, M., Stimm, B., Gunter, S., Palomeque, X., ... Beck, E. (2014). Afforestation or intense pasturing improve the ecological and economic value of abandoned tropical farmlands. *Nature Communications*, *5*, 5612. <https://doi.org/10.1038/ncomms6612>
- Laganiere, J., Angers, D. A., & Pare, D. (2010). Carbon accumulation in agricultural soils after afforestation: A meta-analysis. *Global Change Biology*, *16*, 439–453. <https://doi.org/10.1111/j.1365-2486.2009.01930.x>
- Lai, J., Zou, Y., Zhang, J., & Peres-Neto, P. (2022). Generalizing hierarchical and variation partitioning in multiple regression and canonical analyses using the rdacca.Hp R package. *Methods in Ecology and Evolution*, *00*, 1–7. <https://doi.org/10.1111/2041-210X.13800>
- Leibold, M. A., & McPeck, M. A. (2006). Coexistence of the niche and neutral perspectives in community ecology. *Ecology*, *87*, 1399–1410. [https://doi.org/10.1890/0012-9658\(2006\)87\[1399:COTNAN\]2.0.CO;2](https://doi.org/10.1890/0012-9658(2006)87[1399:COTNAN]2.0.CO;2)
- Leizeaga, A., Hicks, L. C., Manoharan, L., Hawkes, C. V., Rousk, J., & Wilson, G. (2020). Drought legacy affects microbial community trait distributions related to moisture along a savannah grassland precipitation gradient. *Journal of Ecology*, *00*, 1–16. <https://doi.org/10.1111/1365-2745.13550>
- Li, B., Li, P., Zhang, W., Ji, J., Liu, G., & Xu, M. (2021). Deep soil moisture limits the sustainable vegetation restoration in arid and semi-arid loess plateau. *Geoderma*, *399*, 115122. <https://doi.org/10.1016/j.geoderma.2021.115122>
- Liang, M., Johnson, D., Burslem, D. F. R. P., Yu, S., Fang, M., Taylor, J. D., Taylor, A. F. S., Helgason, T., & Liu, X. (2020). Soil fungal networks maintain local dominance of ectomycorrhizal trees. *Nature Communications*, *11*, 2636. <https://doi.org/10.1038/s41467-020-16507-y>
- Liu, Y., Song, H., An, Z., Sun, C., Trouet, V., Cai, Q., Liu, R., Leavitt, S. W., Song, Y., Li, Q., Fang, C., Zhou, W., Yang, Y., Jin, Z., Wang, Y., Sun, J., Mu, X., Lei, Y., Wang, L., ... Zeng, X. (2020). Recent anthropogenic curtailing of Yellow River runoff and sediment load is unprecedented over the past 500 y. *Proceedings of the National Academy of Sciences of the United States of America*, *117*, 18251–18257. <https://doi.org/10.1073/pnas.1922349117>
- Malik, A. A., Swenson, T., Weihe, C., Morrison, E. W., Martiny, J. B. H., Brodie, E. L., Northen, T. R., & Allison, S. D. (2020). Drought and plant litter chemistry alter microbial gene expression and metabolite production. *The ISME Journal*, *14*, 2236–2247. <https://doi.org/10.1038/s41396-020-0683-6>
- McGulley, R. L., Jobbágy, E. G., Pockman, W. T., & Jackson, R. B. (2004). Nutrient uptake as a contributing explanation for deep rooting in arid and semi-arid ecosystems. *Oecologia*, *141*, 620–628. <https://doi.org/10.1007/s00442-004-1687-z>
- Meisner, A., Snoek, B. L., Nesme, J., Dent, E., Jacquiod, S., Classen, A. T., & Prieme, A. (2021). Soil microbial legacies differ following drying–rewetting and freezing–thawing cycles. *The ISME Journal*, *15*, 1207–1221. <https://doi.org/10.1038/s41396-020-00844-3>
- Meisser, M., Vitra, A., Deléglise, C., Dubois, S., Probo, M., Mosimann, E., Buttler, A., & Mariotte, P. (2019). Nutrient limitations induced by drought affect forage N and P differently in two permanent grasslands. *Agriculture, Ecosystems and Environment*, *280*, 85–94. <https://doi.org/10.1016/j.agee.2019.04.027>
- Mo, Y., Peng, F., Gao, X., Xiao, P., Logares, R., Jeppesen, E., Ren, K., Xue, Y., & Yang, J. (2021). Low shifts in salinity determined assembly processes and network stability of microeukaryotic plankton communities in a subtropical urban reservoir. *Microbiome*, *9*, 128. <https://doi.org/10.1186/s40168-021-01079-w>
- Moorhead, D. L., Rinkes, Z. L., Sinsabaugh, R. L., & Weintraub, M. N. (2013). Dynamic relationships between microbial biomass, respiration, inorganic nutrients and enzyme activities: Informing enzyme-based decomposition models. *Frontiers in Microbiology*, *4*, 223. <https://doi.org/10.3389/fmicb.2013.00223>
- Mukhopadhyay, S., & Joy, V. C. (2010). Influence of leaf litter types on microbial functions and nutrient status of soil: Ecological suitability of forest trees for afforestation in tropical laterite wastelands. *Soil Biology and Biochemistry*, *42*, 2306–2315. <https://doi.org/10.1016/j.soilbio.2010.09.007>
- Muyzer, G., de Waal, E. C., & Uitterlinden, A. G. (1993). Profiling of complex microbial populations by denaturing gradient gel electrophoresis analysis of polymerase chain reaction-amplified genes coding for 16S rRNA. *Applied and Environmental Microbiology*, *59*, 695–700. <https://doi.org/10.1128/aem.59.3.695-700.1993>
- Na, X., Yu, H., Wang, P., Zhu, W., Niu, Y., & Huang, J. (2019). Vegetation biomass and soil moisture coregulate bacterial community succession under altered precipitation regimes in a desert steppe in northwestern China. *Soil Biology and Biochemistry*, *136*, 107520. <https://doi.org/10.1016/j.soilbio.2019.107520>
- Navarrete, A. A., Tsai, S. M., Mendes, L. W., Faust, K., de Hollander, M., Cassman, N. A., Raes, J., van Veen, J. A., & Kuramae, E. E. (2015). Soil microbiome responses to the short-term effects of Amazonian deforestation. *Molecular Ecology*, *24*, 2433–2448. <https://doi.org/10.1111/mec.13172>
- Naylor, D., & Coleman-Derr, D. (2017). Drought stress and root-associated bacterial communities. *Frontiers in Plant Science*, *8*, 2223. <https://doi.org/10.3389/fpls.2017.02223>
- Ochoa-Hueso, R., Collins, S. L., Delgado-Baquerizo, M., Hamonts, K., Pockman, W. T., Sinsabaugh, R. L., Smith, M. D., Knapp, A. D., & Power, S. A. (2018). Drought consistently alters the composition of soil fungal and bacterial communities in grasslands from two continents. *Global Change Biology*, *24*, 2818–2827. <https://doi.org/10.1111/gcb.14113>
- Oliveira, R. S., Bezerra, L., Davidson, E. A., Pinto, F., Klink, C. A., Nepstad, D. C., & Moreira, A. (2005). Deep root function in soil water dynamics in cerrado savannas of Central Brazil. *Functional Ecology*, *19*, 574–581. <https://doi.org/10.1111/j.1365-2435.2005.01003.x>
- Plaza, C., Zaccone, C., Sawicka, K., Mendez, A. M., Tarquis, A. M., Gasco, G., Heuvelink, G. B. M., Schuur, E. A. G., & Maestre, F. T. (2018). Soil resources and element stocks in drylands to face global issues. *Scientific Reports*, *8*, 13788. <https://doi.org/10.1038/s41598-018-32229-0>
- Peng, C., Ma, Z., Lei, X., Zhu, Q., Chen, H., Wang, W., Liu, S., Li, W., Fang, X., & Zhou, X. (2011). A drought-induced pervasive increase in tree mortality across Canada's boreal forests. *Nature Climate Change*, *1*, 467–471. <https://doi.org/10.1038/nclimate1293>
- Peng, G. S., & Wu, J. (2016). Optimal network topology for structural robustness based on natural connectivity. *Physica A: Statistical Mechanics and its Applications*, *443*, 212–220. <https://doi.org/10.1016/j.physa.2015.09.023>
- Price, M. N., Dehal, P. S., & Arkin, A. P. (2010). FastTree 2—approximately maximum-likelihood trees for large alignments. *PLoS One*, *5*, e9490. <https://doi.org/10.1371/journal.pone.0009490>
- Qiu, L., Zhang, Q., Zhu, H., Reich, P. B., Banerjee, S., van der Heijden, M. G. A., Sadowsky, M. J., Ishii, S., Jia, X., Shao, M., Liu, B., Jiao, H., Li, H., & Wei, X. (2021). Erosion reduces soil microbial diversity, network complexity and multifunctionality. *The ISME Journal*, *15*, 2474–2489. <https://doi.org/10.1038/s41396-021-00913-1>
- Richter, D. D., Markewitz, D., Trumbore, S. E., & Wells, C. G. (1999). Rapid accumulation and turnover of soil carbon in a re-establishing forest. *Nature*, *400*, 56–58. <https://doi.org/10.1038/21867>
- Schimel, J., Balsler, T. C., & Wallenstein, M. (2007). Microbial stress-response physiology and its implications for ecosystem function. *Ecology*, *88*, 1386–1394. <https://doi.org/10.1890/06-0219>
- Schimel, J. P. (2018). Life in dry soils: Effects of drought on soil microbial communities and processes. *Annual Review of Ecology, Evolution, and*

- Systematics*, 49, 409–432. <https://doi.org/10.1146/annurev-ecolsys-110617-062614>
- Schlaepfer, D. R., Bradford, J. B., Lauenroth, W. K., Munson, S. M., Tietjen, B., Hall, S. A., Wilson, S. D., Duniway, M. C., Jia, G., Pyke, D. A., Lkhagva, A., & Jamiyansharav, K. (2017). Climate change reduces extent of temperate drylands and intensifies drought in deep soils. *Nature Communications*, 8, 14196. <https://doi.org/10.1038/ncomms14196>
- Schlatter, D. C., Kahl, K., Carlson, B., Huggins, D. R., & Paulitz, T. (2020). Soil acidification modifies soil depth-microbiome relationships in a no-till wheat cropping system. *Soil Biology and Biochemistry*, 149, 107939. <https://doi.org/10.1016/j.soilbio.2020.107939>
- Shao, M., Jia, X., Wang, Y., & Zhu, Y. (2016). A review of studies on dried soil layers in the loess plateau. *Advances in Earth Science*, 31, 14–22. <https://doi.org/10.11867/j.issn.1001-8166.2016.01.0014> (in Chinese with English Abstract).
- Shi, Y., Zhang, K., Li, Q., Liu, X., He, J. S., & Chu, H. (2020). Interannual climate variability and altered precipitation influence the soil microbial community structure in a Tibetan plateau grassland. *Science of the Total Environment*, 714, 136794. <https://doi.org/10.1016/j.scitotenv.2020.136794>
- Shiple, B. (2009). Confirmatory path analysis in a generalized multilevel context. *Ecology*, 90, 363–368. <https://doi.org/10.1890/08-1034.1>
- Shiple, B. (2013). The AIC model selection method applied to path analytic models compared using a d-separation test. *Ecology*, 94, 560–564. <https://doi.org/10.1890/12-0976.1>
- Stegen, J. C., Lin, X., Fredrickson, J. K., Chen, X., Kennedy, D. W., Murray, C. J., Rockhold, M. L., & Konopka, A. (2013). Quantifying community assembly processes and identifying features that impose them. *The ISME Journal*, 7, 2069–2079. <https://doi.org/10.1038/ismej.2013.93>
- Stegen, J. C., Lin, X., Fredrickson, J. K., & Konopka, A. E. (2015). Estimating and mapping ecological processes influencing microbial community assembly. *Frontiers in Microbiology*, 6, 370. <https://doi.org/10.3389/fmicb.2015.00370>
- Stegen, J. C., Lin, X., Konopka, A. E., & Fredrickson, J. K. (2012). Stochastic and deterministic assembly processes in subsurface microbial communities. *The ISME Journal*, 6, 1653–1664. <https://doi.org/10.1038/ismej.2012.22>
- Stewart, C. E., Roosendaal, D., Deneff, K., Pruessner, E., Comas, L. H., Sarath, G., Jin, V. L., Schmer, M. R., & Soundararajan, M. (2017). Seasonal switchgrass ecotype contributions to soil organic carbon, deep soil microbial community composition and rhizodeposit uptake during an extreme drought. *Soil Biology and Biochemistry*, 112, 191–203. <https://doi.org/10.1016/j.soilbio.2017.04.021>
- Tripathi, B. M., Stegen, J. C., Kim, M., Dong, K., Adams, J. M., & Lee, Y. K. (2018). Soil pH mediates the balance between stochastic and deterministic assembly of bacteria. *The ISME Journal*, 12, 1072–1083. <https://doi.org/10.1038/s41396-018-0082-4>
- Upton, R. N., Checinska Sielaff, A., Hofmockel, K. S., Xu, X., Polley, H. W., & Wilsey, B. J. (2020). Soil depth and grassland origin cooperatively shape microbial community co-occurrence and function. *Ecosphere*, 11, e02973. <https://doi.org/10.1002/ecs2.2973>
- Wang, L., Wang, Q., Wei, S., Shao, M., & Li, Y. (2008). Soil desiccation for loess soils on natural and regrown areas. *Forest Ecology and Management*, 255, 2467–2477. <https://doi.org/10.1016/j.foreco.2008.01.006>
- Wang, S., Fu, B., Gao, G., Yao, X., & Zhou, J. (2012). Soil moisture and evapotranspiration of different land cover types in the loess plateau, China. *Hydrology and Earth System Sciences*, 16, 2883–2892. <https://doi.org/10.5194/hess-16-2883-2012>
- Wang, S., Fu, B., Piao, S., Lü, Y., Ciais, P., Feng, X., & Wang, Y. (2016). Reduced sediment transport in the Yellow River due to anthropogenic changes. *Nature Geoscience*, 9, 38–41. <https://doi.org/10.1038/ngeo2602>
- Wang, S., Wang, X. B., Han, X. G., & Deng, Y. (2018). Higher precipitation strengthens the microbial interactions in semi-arid grassland soils. *Global Ecology and Biogeography*, 27, 570–580. <https://doi.org/10.1111/geb.12718>
- Wang, Y., Li, C., Tu, B., Kou, Y., & Li, X. (2021). Species pool and local ecological assembly processes shape the β -diversity of diazotrophs in grassland soils. *Soil Biology and Biochemistry*, 160, 108338. <https://doi.org/10.1016/j.soilbio.2021.108338>
- Wang, Z., Liu, B., Liu, G., & Zhang, Y. (2009). Soil water depletion depth by planted vegetation on the loess plateau. *Science in China Series D: Earth Sciences*, 52, 835–842. <https://doi.org/10.1007/s11430-009-0087-y>
- Wei, X., Ma, T., Wang, Y., Wei, Y., Hao, M., Shao, M., & Zhang, X. (2016). Long-term fertilization increases the temperature sensitivity of OC mineralization in soil aggregates of a highland agroecosystem. *Geoderma*, 272, 1–9. <https://doi.org/10.1016/j.geoderma.2016.02.027>
- Wei, X., Qiu, L., Shao, M., Zhang, X., & Gale, W. J. (2012). The accumulation of organic carbon in mineral soils by afforestation of abandoned farmland. *PLoS One*, 7, e32054. <https://doi.org/10.1371/journal.pone.0032054>
- Wu, M., Chen, S., Chen, J., Xue, K., Chen, S., Wang, X., Chen, T., Kang, S., Rui, J., Thies, J. E., Bardgett, R. D., & Wang, Y. (2021). Reduced microbial stability in the active layer is associated with carbon loss under alpine permafrost degradation. *Proceedings of the National Academy of Sciences of the United States of America*, 118, e2025321118. <https://doi.org/10.1073/pnas.2025321118>
- Xu, L., He, N., Li, X., Cao, H., Li, C., Wang, R., Wang, C., Yao, M., Zhou, S., & Wang, J. (2021). Local community assembly processes shape β -diversity of soil phoD-harboring communities in the northern hemisphere steppes. *Global Ecology and Biogeography*, 00, 1–13. <https://doi.org/10.1111/geb.13385>
- Yang, L., Wei, W., Chen, L., Jia, F., & Mo, B. (2012). Spatial variation of shallow and deep soil moisture in the semi-arid loess hilly area, China. *Hydrology and Earth System Sciences*, 9, 4553–4586. <https://doi.org/10.5194/hess-16-3199-2012>
- Yao, Y., Ge, N., Yu, S., Wei, X., Wang, X., Jin, J., Liu, X., Shao, M., Wei, Y., & Kang, L. (2019). Response of aggregate associated organic carbon, nitrogen and phosphorous to re-vegetation in agro-pastoral ecotone of northern China. *Geoderma*, 341, 172–180. <https://doi.org/10.1016/j.geoderma.2019.01.036>
- Yin, R., Deng, H., Wang, H., & Zhang, B. (2014). Vegetation type affects soil enzyme activities and microbial functional diversity following re-vegetation of a severely eroded red soil in sub-tropical China. *Catena*, 115, 96–103. <https://doi.org/10.1016/j.catena.2013.11.015>
- Yu, Y., Lee, C., Kim, J., & Hwang, S. (2005). Group-specific primer and probe sets to detect methanogenic communities using quantitative real-time polymerase chain reaction. *Biotechnology and Bioengineering*, 89, 670–679. <https://doi.org/10.1002/bit.20347>
- Zhong, Z., Li, W., Lu, X., Gu, Y., Wu, S., Shen, Z., Han, X., Yang, G., & Ren, C. (2020). Adaptive pathways of soil microorganisms to stoichiometric imbalances regulate microbial respiration following afforestation in the loess plateau, China. *Soil Biology and Biochemistry*, 151, 108048. <https://doi.org/10.1016/j.soilbio.2020.108048>

SUPPORTING INFORMATION

Additional supporting information can be found online in the Supporting Information section at the end of this article.

How to cite this article: Kong, W., Wei, X., Wu, Y., Shao, M., Zhang, Q., Sadowsky, M. J., Ishii, S., Reich, P. B., Wei, G., Jiao, S., Qiu, L., & Liu, L. (2022). Afforestation can lower microbial diversity and functionality in deep soil layers in a semiarid region. *Global Change Biology*, 28, 6086–6101. <https://doi.org/10.1111/gcb.16334>